**Smart Structures and Systems**, *Vol. 13, No. 5 (2014) 797-819*
DOI: http://dx.doi.org/10.12989/sss.2014.13.5.797 

# Constructing the mode shapes of a bridge from a passing vehicle: a theoretical study

Y.B. Yang*[1], Y.C. Li[1] and K.C. Chang[2]

[1]*Department of Civil Engineering, National Taiwan University, Taipei, Taiwan 10617*
[2]*Department of Civil and Earth Resources Engineering, Kyoto University, Kyoto 606-8501, Japan*

*(Received March 26, 2012, Revised May 25, 2013, Accepted August 22, 2013)*

**Abstract.** This paper presents a theoretical algorithm for constructing the mode shapes of a bridge from the dynamic responses of a test vehicle moving over the bridge. In comparison with those approaches that utilize a limited number of sensors deployed on the bridge, the present approach can offer much more spatial information, as well as higher resolution in mode shapes, since the test vehicle can receive the vibration characteristics of each point during its passage on the bridge. Basically only one or few sensors are required to be installed on the test vehicle. Factors that affect the accuracy of the present approach for constructing the bridge mode shapes are studied, including the vehicle speed, random traffic, and road surface roughness. Through numerical simulations, the present approach is verified to be feasible under the condition of constant and low vehicle speeds.

**Keywords:** mode shape identification; test vehicle; instantaneous amplitude; vehicle-bridge interaction

## 1. Introduction

Measuring the mode shapes of a bridge is a crucial task in bridge engineering, since the measured mode shapes serve as useful indexes for many applications related to bridges, such as numerical model calibration and updating (Brownjohn *et al*. 2001, Jaishi and Ren 2005, Altunisik *et al*. 2012), structural health monitoring and damage detection (Doebling *et al*. 1998, Farrar *et al*. 2001, Chang *et al*. 2003, Carden and Fanning 2004, Chrysostomou *et al*. 2008), and so on. Conventionally, to measure the mode shapes of a bridge, quite a number of sensors should be mounted on the bridge deck to record the dynamic responses of the bridge under certain sources of vibration. Then, the mode shapes of the bridge can be identified by performing system identification and/or data processing techniques on the recorded bridge responses, as well as the vibration source histories in some cases where they are available. Details for such modal identification approaches are available in many references, e.g., the books by Ewins (2000) and Wenzel and Pichler (2005) and the papers by Farrar and James (1997) and Huang *et al.* (1999).The number and locations of the sensors may vary from case to case, depending upon the engineers' judgment on the trade-off between the spatial resolution and experiment cost. Generally, to

*Corresponding author, Professor, E-mail: ybyang@ntu.edu.tw


http://www.techno-press.org/?journal=sss&subpage=8 ISSN: 1738-1584 (Print), 1738-1991 (Online)

guarantee higher spatial resolution for mode shapes requires a larger number of sensors to be mounted, which is accompanied by higher consumption of cost, time, and labor.

Yang *et al*. (2004) presented a novel idea for extracting the dynamic characteristics of a bridge indirectly from the dynamic response of a test vehicle during its passage over a bridge, rather than from the dynamic response of the bridge. This approach requires only few sensors to be installed on the moving vehicle, but no sensors on the bridge, showing its relative advantage for fast scanning the bridge dynamic characteristics. Such an approach has been referred to as the *indirect approach*, in comparison with the conventional approaches that are regarded as the *direct approach*. Recently, the indirect approaches have been extended to various applications related to bridges, such as frequency extraction (Yang and Lin 2005, Yang and Chang 2009),damage detection (Bu *et al*. 2006, McGetrick *et al*. 2009), and other relevant issues (Yin and Tang 2011).

Recently, Zhang *et al*. (2012) attempted to extend the indirect approach to extraction of mode-shape-related dynamic characteristics of a bridge and verified its feasibility numerically and experimentally. They utilized a passing vehicle equipped with tapping devices to extract the approximate mode shape squares of the bridge, for the purpose of damage detection. Contradiction was induced between the frequency and spatial resolutions, namely, better result is obtained for the former using longer analysis time intervals, but not for the latter, due to the use of short-time Fourier transform as their major data processing tool. Such an attempt is encouraging in that it reveals an additional advantage of the indirect approach: high spatial resolution in the extracted mode shapes. The passing vehicle, which is also designated as the test vehicle, can receive the vibration characteristics of every point it has traveled over the bridge. In comparison with the direct approaches that have a limited number of sensors deployed on the bridge, the indirect approach can offer more spatial information, as well as higher resolution in mode shapes.

The objective of this paper is to present an indirect approach for extracting the mode shapes of a bridge with high spatial resolutions from the dynamic response of a passing test vehicle. To reduce the contradiction mentioned above, while achieving the highest resolution in the longitudinal spatial domain, the concept of instantaneous amplitudes, obtained as a result of the Hilbert transform, will be introduced in the following section. Then, the theoretical formulation for the present approach will be given in detail, followed by its operating algorithms and constraints. Through four numerical cases, the feasibility of the present approach is illustrated and the factors that affect the accuracy of the extracted mode shapes are studied.

## 2. Hilbert transform (HT)

Given a time series $s(t)$, the Hilbert transform (HT) of $s(t)$ is defined as (Bandat and Piersol 1986)

$$\hat{s}(t) = \mathbf{H}\left(s(t)\right) = \frac{1}{\pi} \boldsymbol{PV} \int_{-\infty}^{\infty} \frac{s(\tau)}{t-\tau} d\tau \tag{1}$$

where ***PV*** denotes the Cauchy principal value. The HT of $s(t)$ can be interpreted as the convolution of $s(t)$ with a unit impulse function of $1/\pi t$, thus it preserves most local information of $s(t)$. Then, $s(t)$ and $\hat{s}(t)$ can form an analytical function $z(t)$ as

$$z(t) = s(t) + i\hat{s}(t) \tag{2}$$

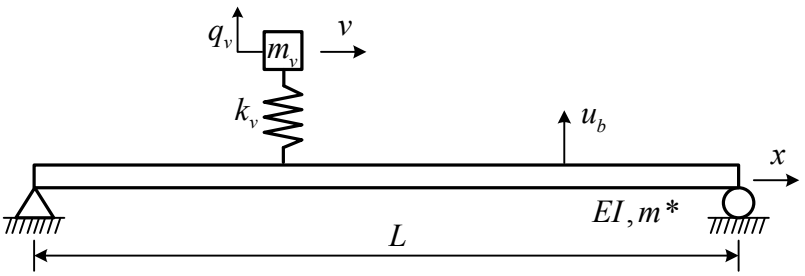


Fig. 1 Mathematical model of a test vehicle moving on a bridge

Mapping $z(t)$ from the complex Cartesian coordinates to polar coordinates yields

$$z(t) = A(t)e^{i\theta(t)} \tag{3}$$

where

$$A(t) = \sqrt{s^2(t) + \hat{s}^2(t)}, \quad \theta(t) = \arctan\left(\frac{\hat{s}(t)}{s(t)}\right) \tag{4, 5}$$

The time-dependent function $A(t)$ is referred to as the instantaneous amplitude function of the original function $s(t)$, and $\theta(t)$ as the instantaneous phase function. In addition, the instantaneous amplitude function $A(t)$ can be regarded as the envelope function of $s(t)$. The above definitions for the instantaneous amplitude and phase functions are physically meaningful only when the time series is "mono-component" or "narrow-band" (Huang *et al*. 1998, Huang *et al*. 1999).

## 3. Theoretical formulation

Fig. 1 shows the mathematical model of a test vehicle moving on a simple bridge. In this model, the vehicle is simplified as a moving sprung mass $m_v$, supported by a spring of stiffness $k_v$; the bridge is a simply-supported beam of length $L$, constant mass density $m^*$ per unit length, and constant bending rigidity $EI$. To focus on the physical meanings of the vehicle response, the following assumptions are adopted without losing the generality of the problem: (1) Road surface roughness is ignored in the derivation, but will be included in one of the numerical cases studied later on to evaluate its impact. (2) Vehicle mass is negligibly small in comparison with the bridge mass. (3) Before the arrival of the test vehicle, the bridge remains at rest, i.e., zero initial conditions are assumed for the bridge. This assumption is reasonable because the bridge vibrations caused by ambient excitations are generally small enough to be ignored in comparison with those by moving vehicular loads. (4) Damping is neglected for both the vehicle and bridge. This assumption is also reasonable because the vibrations of both the vehicle and bridge under the moving vehicle action are forced vibrations, for which the role of damping is insignificant. (5) The test vehicle travels at constant speed $v$ during its passage over the bridge.

The equations of motion can be written for the vehicle and bridge as follows

$$m_v\ddot{q}_v(t)+k_v(q_v(t)-u(x,t)\big|_{x=vt})=0 \tag{6}$$

$$m^*\ddot{u}(x,t)+EIu''''(x,t)=f_c(t)\delta(x-vt) \tag{7}$$

where $u(x,t)$ denotes the vertical displacement of the bridge, $q_v(t)$ the vertical displacement of the vehicle, measured from its static equilibrium position, and a dot and a prime represents the derivative with respect to time $t$ and longitudinal coordinate $x$, respectively. The contact force $f_c(t)$ can be expressed as

$$f_c(t)=-m_v g+k_v\left(q_v(t)-u(x,t)\big|_{x=vt}\right) \tag{8}$$

where $g$ is the gravitational acceleration.

Using the modal superposition method, i.e., expressing the bridge displacement response $u(x,t)$ in terms of modal shapes $\sin(n\pi x/L)$ and generalized coordinates $q_{b,n}(t)$,

$$u(x,t)=\sum_{n=1}^{\infty}\sin\frac{n\pi x}{L}q_{b,n}(t) \tag{9}$$

one can obtain the solution of the displacement response of the test vehicle as (Yang and Lin 2005, Yang and Chang 2009)

$$\begin{aligned}q_v(t)=\sum_{n=1}^{\infty}\{&A_{1,n}\cos\left(\frac{(n-1)\pi v}{L}\right)t+A_{2,n}\cos\left(\frac{(n+1)\pi v}{L}\right)t+A_{3,n}\cos(\omega_v t)\\&+A_{4,n}\cos\left(\omega_{b,n}-\frac{n\pi v}{L}\right)t+A_{5,n}\cos\left(\omega_{b,n}+\frac{n\pi v}{L}\right)t\}\end{aligned} \tag{10}$$

where the coefficient of each term is

$$A_{1,n}=\frac{\Delta_{st,n}\omega_v^2}{2(1-S_n^2)\left(\omega_v+\frac{(n-1)\pi v}{L}\right)\left(\omega_v-\frac{(n-1)\pi v}{L}\right)} \tag{11}$$

$$A_{2,n}=\frac{-\Delta_{st,n}\omega_v^2}{2(1-S_n^2)\left(\omega_v+\frac{(n+1)\pi v}{L}\right)\left(\omega_v-\frac{(n+1)\pi v}{L}\right)} \tag{12}$$

$$A_{3,n}=\frac{2\Delta_{st,n}\omega_v^2\left(\frac{\pi v}{L}\right)^2 n}{2\left(1-S_n^2\right)\left(\omega_v+\frac{(n-1)\pi v}{L}\right)\left(\omega_v-\frac{(n-1)\pi v}{L}\right)\left(\omega_v+\frac{(n+1)\pi v}{L}\right)\left(\omega_v-\frac{(n+1)\pi v}{L}\right)}$$
$$-\frac{2\Delta_{st,n}S_n\omega_v^2\left(\frac{n\pi v}{L}\right)\omega_{b,n}}{\left(\omega_v-\omega_{b,n}+\frac{n\pi v}{L}\right)\left(\omega_v+\omega_{b,n}-\frac{n\pi v}{L}\right)\left(\omega_v+\omega_{b,n}+\frac{n\pi v}{L}\right)\left(\omega_v-\omega_{b,n}-\frac{n\pi v}{L}\right)} \tag{13}$$

$$A_{4,n}=\frac{-S_n\Delta_{st,n}\omega_v^2}{2\left(1-S_n^2\right)\left(\omega_v-\omega_{b,n}+\frac{n\pi v}{L}\right)\left(\omega_v+\omega_{b,n}-\frac{n\pi v}{L}\right)} \tag{14}$$

$$A_{5,n}=\frac{S_n\Delta_{st,n}\omega_v^2}{2\left(1-S_n^2\right)\left(\omega_v+\omega_{b,n}+\frac{n\pi v}{L}\right)\left(\omega_v-\omega_{b,n}-\frac{n\pi v}{L}\right)} \tag{15}$$

and the vehicle frequency $\omega_v$, bridge frequency $\omega_{b,n}$, vehicle-induced static deflection $\Delta_{st,n}$ of the bridge, and the speed parameter $S_n$, of the $n$-th mode are defined as

$$\omega_v=\sqrt{\frac{k_v}{m_v}} \tag{16}$$

$$\omega_{b,n}=\frac{n^2\pi^2}{L^2}\sqrt{\frac{EI}{m^*}} \tag{17}$$

$$\Delta_{st,n}=\frac{-2m_vgL^3}{n^4\pi^4EI} \tag{18}$$

$$S_n=\frac{n\pi v}{L\omega_{b,n}} \tag{19}$$

The bridge response can also be solved in a similar manner (Yang and Lin 2005, Yang and Chang 2009). However, it won't be presented herein since it is not of concern in this study.

Taking the derivative of the vehicle displacement response twice, one can obtain the vehicle acceleration response as

$$\ddot{q}_v(t)=\sum_{n=1}^{\infty}\{\bar{\bar{A}}_{1,n}\cos\left(\frac{(n-1)\pi v}{L}\right)t+\bar{\bar{A}}_{2,n}\cos\left(\frac{(n+1)\pi v}{L}\right)t+\bar{\bar{A}}_{3,n}\cos(\omega_v t)$$
$$+\bar{\bar{A}}_{4,n}\cos\left(\omega_{b,n}-\frac{n\pi v}{L}\right)t+\bar{\bar{A}}_{5,n}\cos\left(\omega_{b,n}+\frac{n\pi v}{L}\right)t\} \tag{20}$$

with the coefficients as

$$\ddot{\bar{A}}_{1,n} = -\left(\frac{(n-1)\pi v}{L}\right)^2 \times A_{1,n},\ \ddot{\bar{A}}_{2,n} = -\left(\frac{(n+1)\pi v}{L}\right)^2 \times A_{2,n},\ \ddot{\bar{A}}_{3,n} = -\omega_v^2 \times A_{3,n},$$
$$\ddot{\bar{A}}_{4,n} = -\left(\omega_{b,n} - \frac{n\pi v}{L}\right)^2 \times A_{4,n},\ \ddot{\bar{A}}_{5,n} = -\left(\omega_{b,n} + \frac{n\pi v}{L}\right)^2 \times A_{5,n} \tag{21}$$

Clearly, the vehicle response is dominated by five frequencies, i.e., the left-shifted driving frequency $(n\text{-}1)\pi v/L$, right-shifted driving frequency $(n+1)\pi v/L$, vehicle frequency $\omega_v$, left-shifted bridge frequency $\omega_{b,n}\text{-}n\pi v/L$, and right-shifted bridge frequency $\omega_{b,n}+n\pi v/L$.

To extract the mode shapes of the bridge, the component response corresponding to the bridge frequency of the $n$-th mode should be singled out from the vehicle response by a feasible filtering technique. According to Eq. (20), the extracted bridge component response $R_b$ associated with the $n$-th mode is

$$R_b = A_l \cos\left(\omega_{b,n} - \frac{n\pi v}{L}\right)t + A_r \cos\left(\omega_{b,n} + \frac{n\pi v}{L}\right)t \tag{22}$$

where the coefficients $A_l$ and $A_r$ corresponding to the left- and right-shifted bridge frequencies are

$$A_l = \ddot{\bar{A}}_{4,n} = \left(\omega_{b,n} - \frac{n\pi v}{L}\right)^2 \frac{S_n \Delta_{st,n} \omega_v^2}{2\left(1 - S_n^2\right)\left(\omega_v - \omega_{b,n} + \frac{n\pi v}{L}\right)\left(\omega_v + \omega_{b,n} - \frac{n\pi v}{L}\right)} \tag{23}$$

$$A_r = \ddot{\bar{A}}_{5,n} = -\left(\omega_{b,n} + \frac{n\pi v}{L}\right)^2 \frac{S_n \Delta_{st,n} \omega_v^2}{2\left(1 - S_n^2\right)\left(\omega_v - \omega_{b,n} + \frac{n\pi v}{L}\right)\left(\omega_v + \omega_{b,n} - \frac{n\pi v}{L}\right)} \tag{24}$$

The bridge component response $R_b$ is a narrow-band time series and thus can be processed by the HT to yield its transform pair,

$$\hat{R}_b(t) = \mathbf{H}\left[R_b(t)\right] = A_l \sin\left(\omega_{b,n} - \frac{n\pi v}{L}\right)t + A_r \sin\left(\omega_{b,n} + \frac{n\pi v}{L}\right)t \tag{25}$$

From Eq. (4), the instantaneous amplitude of $R_b$ can be obtained as

$$\begin{aligned} A(t) &= \sqrt{R_b^2(t) + \hat{R}_b^2(t)} \\ &= \sqrt{A_l^2 + A_r^2 + 2A_l A_r \cos\left(\frac{2n\pi v t}{L}\right)} \\ &= \sqrt{\left(A_l + A_r\right)^2 - 4A_l A_r \sin^2 \frac{n\pi v t}{L}} \end{aligned} \tag{26}$$

In general, the driving frequency $n\pi v/L$ is much smaller than the bridge frequency $\omega_{b,n}$. Accordingly, the coefficients $A_l$ and $A_r$ in Eqs. (23) and (24)reduce to the following:

$$A_l = \left(\omega_{b,n}\right)^2 \frac{S_n \Delta_{st,n} \omega_v^2}{2\left(1-S_n^2\right)\left(\omega_v - \omega_{b,n}\right)\left(\omega_v + \omega_{b,n}\right)} \tag{27}$$

$$A_r = -\left(\omega_{b,n}\right)^2 \frac{S_n \Delta_{st,n} \omega_v^2}{2\left(1-S_n^2\right)\left(\omega_v - \omega_{b,n}\right)\left(\omega_v + \omega_{b,n}\right)} \tag{28}$$

As can be seen, the two coefficients $A_l$ and $A_r$ are equal in magnitude, but opposite in sign, i.e., $A_l + A_r$=0. Hence, Eq. (26) reduces to

$$A(t) = \sqrt{-4A_l A_r \sin^2 \frac{n\pi vt}{L}} = A_m \left|\sin \frac{n\pi vt}{L}\right| \tag{29}$$

where

$$A_m = \sqrt{-4A_l A_r} = \frac{\omega_{b,n}^2 S_n \Delta_{st,n} \omega_v^2}{\left(1-S_n^2\right)\left|\omega_v^2 - \omega_{b,n}^2\right|} \tag{30}$$

Replacing $x$ with $vt$ in Eq. (29) yields

$$A\left(\frac{x}{v}\right) = A_m \left|\sin \frac{n\pi x}{L}\right| \tag{31}$$

The preceding equation shows that the instantaneous amplitude history $A(x/v)$ of the extracted component response is the mode shape functions sin $(n\pi x/L)$ of the bridge (in absolute value) multiplied by a coefficient $A_m$. A closer look at $A_m$ given in Eq. (30) reveals that it is a function of the speed parameter $S_n$, static deflection $\Delta_{st,n}$, vehicle frequency $\omega_v$, and bridge frequency $\omega_{b,n}$. All these variables are constants, so is $A_m$ a constant. Particularly, the product of the mode shape function and any constant is known to remain a mode shape. The implication here is that, once the component response corresponding to the bridge frequency of a certain mode can be decomposed from the response of the test vehicle during its passage over the bridge, the instantaneous amplitude history of the decomposed component response is representative of the mode shape of concern of the bridge. Theoretically, the mode shapes of the bridge can be extracted with a very high resolution since each point of the bridge has been traveled by the test vehicle.

## 4. Algorithms and constraints

Substituting Eqs. (22) and (25) into Eq. (5), the instantaneous phase $\theta(t)$ can be derived as

$$\theta(t) = \arctan\left(\frac{\hat{R}_b(t)}{R_b(t)}\right) = \arctan\left(-\cot\omega_{b,n}t\right) = \omega_{b,n}t - \frac{\pi}{2} \tag{32}$$

By substituting the expressions for the instantaneous amplitude in Eq. (29) and instantaneous phase in Eq. (32) into Eq. (3), the analytical function can be expressed as follows

$$z(t) = A(t)e^{i\theta(t)} = \left[\frac{\omega_{b,n}^2 S_n \Delta_{st,n}\omega_v^2}{\left(1-S_n^2\right)\left(\omega_v^2-\omega_{b,n}^2\right)}\left|\sin\frac{n\pi vt}{L}\right|\right]e^{i\left(\omega_{b,n}t-\frac{\pi}{2}\right)} \tag{33}$$

The preceding equation indicates that, in the dynamic response of the test vehicle during its passage over the bridge, the component response of the bridge frequency $\omega_{b,n}$ of the $n$-th mode oscillates with a varying amplitude, but with a shape identical to that of the $n$-th mode shape of the bridge in sinusoidal form. Therefore, the bridge component response will oscillate within the envelope formed by the mode shape of the bridge. To sketch the envelope of the bridge component response is equivalent to calculating the instantaneous amplitude.

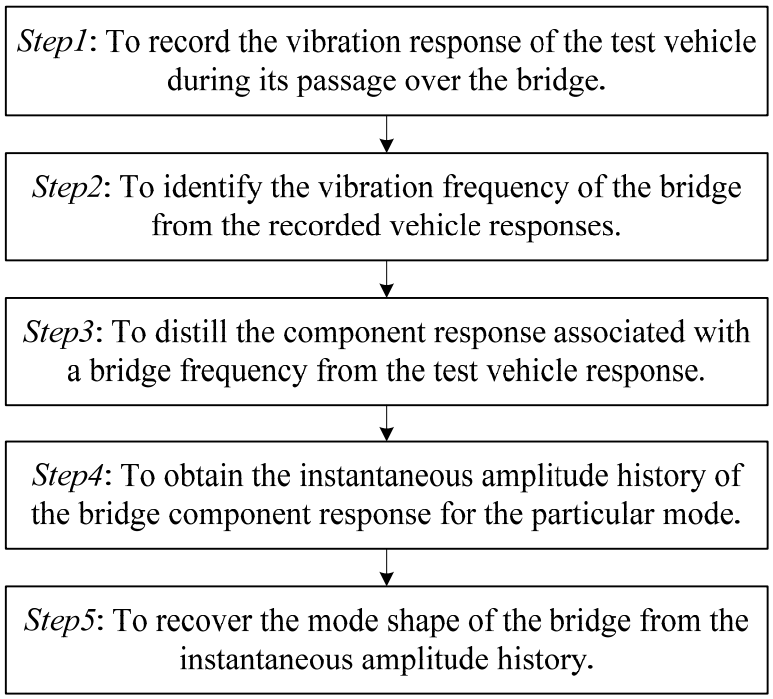


Fig. 2 Flow chart

The procedural steps proposed for extracting the bridge mode shape from the dynamic response of a test vehicle are as follows (see Fig. 2):

*Step 1*: To record the vibration response $R(t)$ of the test vehicle during its passage over the bridge. In practice, the acceleration response of the test vehicle can be measured using the accelerometers (say for seismic use) mounted on the vehicle. The recording interval should cover the whole duration of passage of the test vehicle, i.e., from the instant of entrance to the instant of departure from the bridge. The passing speed should be made as low as possible.

*Step 2*: To identify the vibration frequency $\omega_{b,n}$ of the bridge from the recorded vehicle response $R(t)$. This step can be carried out using any feasible means of identification technique, such as the Fourier transform (Yang *et al*. 2004, McGetrick *et al*. 2009), Fourier transform collaborating with the empirical mode decomposition (EMD) pre-processing technique (Yang and Chang 2009), and so on.

*Step 3*: To extract the component response associated with a bridge frequency from the test vehicle response. After the bridge frequency $\omega_{b,n}$ is made available, one can extract the bridge component response $R_{b,n}(t)$ associated with $\omega_{b,n}$ from the test vehicle response $R(t)$, by any feasible signal processing tools, such as the band-pass filters, singular spectrum analysis, and so on.

*Step 4*: To obtain the instantaneous amplitude history of the bridge component response for the particular mode. Performing the Hilbert transform, as defined in Eq. (1), to the decomposed bridge component response $R_{b,n}(t)$ yields its transform pair $\hat{R}_{b,n}(t)$. Then, one can obtain the instantaneous amplitude history $A_n(t)$ of the bridge component response using Eq. (4).

*Step 5*: To recover the mode shape of the bridge from the instantaneous amplitude history. The curve of the instantaneous amplitude function $A_n(t)$ is representative of the mode shape of the bridge in absolute value. The sign of the mode shape can be decided according to engineers' judgment or experience (Fang and Perera 2009). Note that a discontinuity may appear at common nodes where the signs at both sides of the nodes are forced to be opposite. Finally, the mode shape of the bridge obtained can be normalized or smoothed for any further engineering applications, in a way similar to those processed by other approaches.

With the procedural steps outlined above, the present approach for extracting the mode shape of a bridge is subject to some restraints. One is imposed by the requirement of constant vehicle speed. If the vehicle speed is not constant, the coefficient $A_m$ in Eq. (30) for the instantaneous amplitude history will not remain constant anymore. Consequently, the instantaneous amplitude will deviate from the theoretical mode shape of the bridge in those non-constant speed intervals. The level of deviation will be explored quantitatively as follows.

Suppose that the vehicle speed deviates from the original constant speed with a ratio of $\alpha$ at a certain instant, and so does the speed parameter $S_n$, the coefficient $A_m$ accordingly will vary as follows:

$$A_m(\alpha) = \frac{\alpha\omega_{b,n}^2 S_n \Delta_{st,n} \omega_v^2}{\left(1-\alpha^2 S_n^2\right)\left(\omega_v^2 - \omega_{b,n}^2\right)} \tag{34}$$

The ratio $R_A$ of the varying coefficient $A_m(\alpha)$ to the original constant coefficient $A_m(1)$ can be computed as

$$R_A = \frac{A_m(\alpha)}{A_m(1)} = \frac{\alpha \Big/ \left(1-\alpha^2 S_n^2\right)}{1 \Big/ \left(1-S_n^2\right)} = \frac{\alpha\left(1-S_n^2\right)}{\left(1-\alpha^2 S_n^2\right)} \tag{35}$$

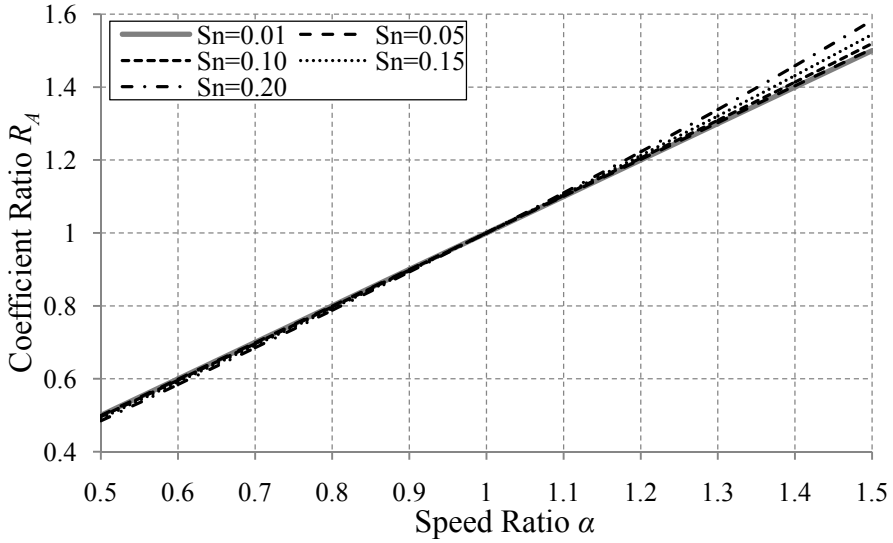


Fig. 3 Coefficient ratio RA vs. speed ratio α

Fig. 3 shows the coefficient ratio $R_A$ with respect to the speed ratio $\alpha$ for the speed parameters $S_n$ =0.01, 0.05, 0.10, 0.15, and 0.20. It is observed that, for small $S_n$ values, say less than 0.15, $R_A$ is approximately equal to $\alpha$ within the interval of small speed variation, say $\alpha$ = 0.6-1.3. For this case, when the varying vehicle speed is $\alpha$ times the original constant speed, the coefficient $A_m$ is approximately equal to $\alpha$ times the theoretical value of the mode shape at that point. Such an observation is useful in retrieving the mode shape from a deviated mode shape, once the varying speed history is recorded as well. Thus, the restraint on the constant vehicle speed can be relaxed and a slightly non-constant vehicle speed is allowed.

Another restraint is imposed by the assumption that the driving frequency $n\pi v/L$ is negligibly smaller than the bridge frequency $\omega_{b,n}$. If the above assumption is violated, the instantaneous amplitude history given in Eq. (26) cannot be reduced to Eq. (29), accompanied by the fact that the instantaneous amplitude history is not a representative mode shape anymore. To evaluate the range of restraint quantitatively, the assumption is removed herein and Eq. (26) is re-derived into a form similar to Eq. (29) as follows:

$$\begin{aligned} A(t) &= \sqrt{\left(A_l + A_r\right)^2 - 4A_l A_r \sin^2 \frac{n\pi vt}{L}} \\ &= \sqrt{1 - \frac{\left(A_l + A_r\right)^2}{A_l A_r \sin^2 \frac{n\pi vt}{L}}} \sqrt{-4A_l A \sin^2 \frac{n\pi vt}{L}} \\ &= R_m A_m \left| \sin \frac{n\pi vt}{L} \right| \end{aligned} \tag{36}$$

where $A_m$ has been defined in Eq. (30) and $R_m$ is the amplification factor of the instantaneous amplitude history, given as

$$R_m = \sqrt{1 - \frac{\left(A_l + A_r\right)^2}{A_l A_r \sin^2 \dfrac{n\pi vt}{L}}} \tag{37}$$

If the assumption of $A_l + A_r = 0$ is valid, the amplification factor $R_m$ will reduce to unity and the instantaneous amplitude history is a representative mode shape of the bridge, which is the case discussed in Sec.3. If the assumption is invalid, $R_m$ can be derived by substituting the expression of $A_l$ and $A_r$ in Eqs. (27) and (28) into Eq. (38), namely

$$R_m = \sqrt{1 + \frac{16S_n^2}{\left(1 - S_n^2\right)^2 \sin^2 \dfrac{n\pi vt}{L}}} \tag{38}$$

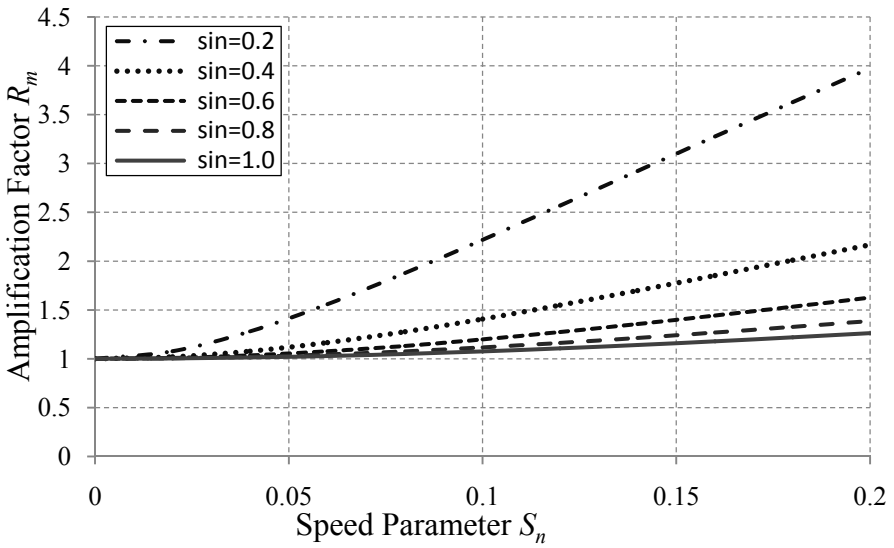


Fig. 4 Amplification factor $R_m$ vs. speed parameter $S_n$.

Fig. 4 shows the amplification factor $R_m$ with respect to the speed parameter $S_n$ for the values of $\sin(n\pi v/L)$ = 0.2, 0.4, 0.6, 0.8, and 1.0. For the general case with $S_n$ approaching 0, as is the case implied by the assumption that the driving frequency $n\pi v/L$ is much smaller than the bridge frequency $\omega_{b,n}$, $R_m$ approximately equals unity. As $S_n$ increases, $R_m$ increases monotonously and therefore deviates from unity, indicating that the instantaneous amplitude history may deviate more from the theoretical mode shape of the bridge as the vehicle speed becomes larger. Moreover, the smaller the value of $\sin(n\pi v/L)$, the more the $R_m$ factor deviates from unity, given the same $S_n$ value.

This means that the $R_m$ factor is sensitive in small $\sin(n\pi v/L)$ intervals, say in the vicinity of nodal points, and non-sensitive in large $\sin(n\pi v/L)$ intervals, say in the vicinity of peaks or troughs of the mode shape. For the purpose of accuracy, it is suggested that the test vehicle be allowed to move at low speeds. If the low speed condition is not met, one can also retrieve the theoretical mode shape from the deviated mode shape making use of the calculated amplification factor.

## 5. Case studies

In order to verify the feasibility of and to understand the restraints of the present approach for extracting the mode shapes of a bridge from the dynamic responses of the passing test vehicle, four numerical cases are studied herein using the finite element simulations. The finite element simulating algorithm utilized in this study is a well-developed vehicle-bridge interaction algorithm (Yang and Yau 1997, Yang *et al*. 2004b). For the cases considered, the following properties are adopted for the simply supported bridge: length $L$ = 30 m, Young's modulus $E$= 27.5 GPa, moment of inertia $I$ = 0.175 m$^4$, and mass density $m^*$ = 1000 kg/m; and the following for the test vehicle: mass $m_v$ = 1000 kg and stiffness $k_v$ = 170 kN/m. The bridge is discretized into 20 identical beam elements, and the time step is selected as 0.001 sec.

In the following, the acceleration responses generated of the test vehicle during its passage over the bridge will be processed with the procedural steps outlined previously to extract the mode shapes of the bridge. The accuracy of the extracted mode shapes is evaluated by the modal assurance criteria (MAC) defined as

$$\text{MAC} = \frac{\phi_e^T \phi_t}{|\phi_e||\phi_t|} \tag{39}$$

where $\phi_e$ and $\phi_t$ denote the extracted and theoretical mode shapes, respectively. Several factors, such as the test vehicle speed, random traffic, and road surface roughness, will be studied as well.

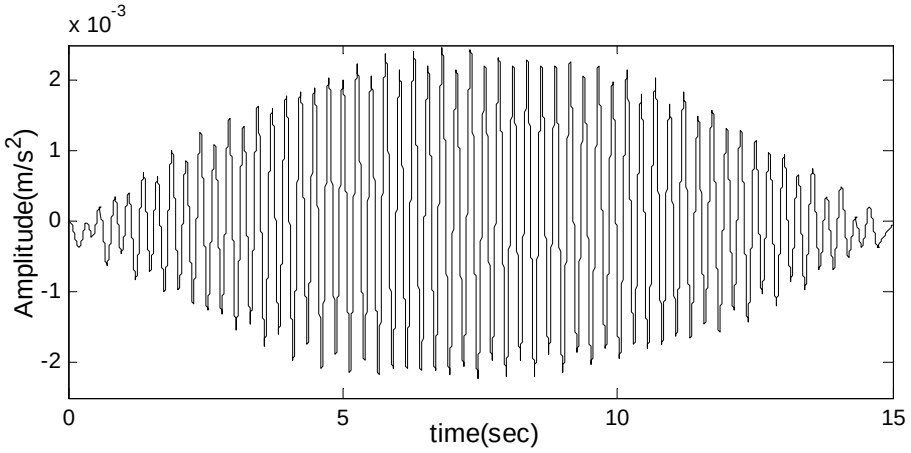


Fig. 5 Acceleration response of the test vehicle

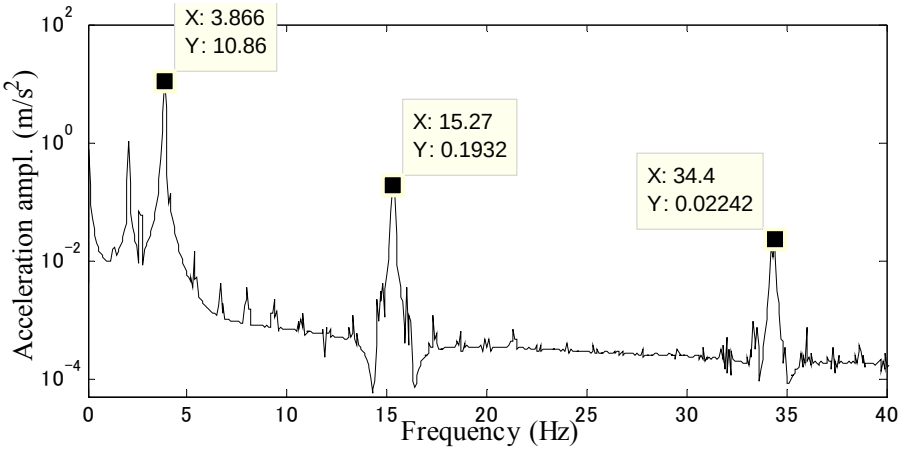


Fig. 6 Acceleration spectrum of the test vehicle

### *5.1. Test vehicle passing through a bridge with smooth road surface*

The first case is to illustrate the present algorithm for extracting the mode shape of the bridge, while verifying its feasibility. In this case, a smooth road surface is considered for the bridge. In the first step, the acceleration response of the test vehicle during its passage of the bridge is generated, as shown in Fig. 5. In the second step, the vehicle response is processed by the fast Fourier transform (FFT) to yield the frequency spectrum as shown in Fig. 6. From this figure, the first three frequencies of the bridge can be identified as 3.87, 15.27, and 34.40 Hz. In the third step, by the conventional band-pass filters, the component responses that correspond to the identified bridge frequencies are decomposed from the test vehicle response, as shown in Fig. 7. It is observed that the component responses oscillate with varying amplitudes that are similar to the respective mode shapes of the bridge. In the fourth step, the Hilbert transform is performed to the bridge component responses to obtain the instantaneous amplitude histories. Finally, one can determine the signs of the mode shapes based on engineering experiences, and obtain the mode shapes of the bridge as in Fig. 8. In comparison with the theoretical mode shapes, the mode shapes identified herein show a high level of accuracy for the case studied.

### *5.2 Effect of vehicle speed*

In this case, the effect of the vehicle speed on the extracted mode shapes of the bridge is studied for three different vehicle speeds: $v$ = 2, 4, and 8 m/s. The bridge remains identical to that studied previously. By following the same procedure, the mode shapes of the bridge can be extracted for each vehicle speed, as shown in Fig. 9. Table 1 lists the MAC values between the extracted mode shapes and theoretical ones. The effect of vehicle speed on the extracted mode shapes can be clearly observed from Fig. 9 and Table 1.

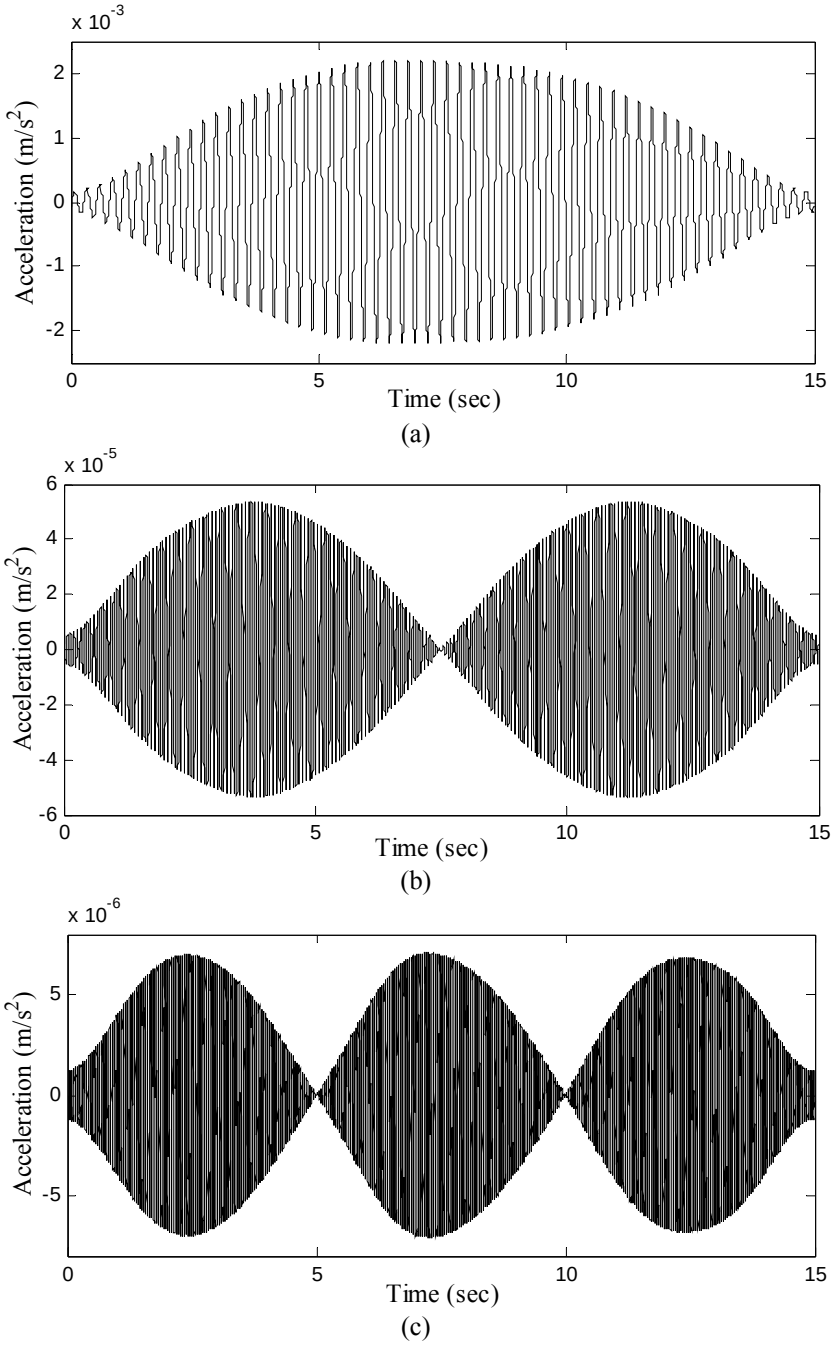


Fig. 7 Component responses of the bridge frequencies: (a) 1st mode, (b) 2nd mode and (c) 3rd mode

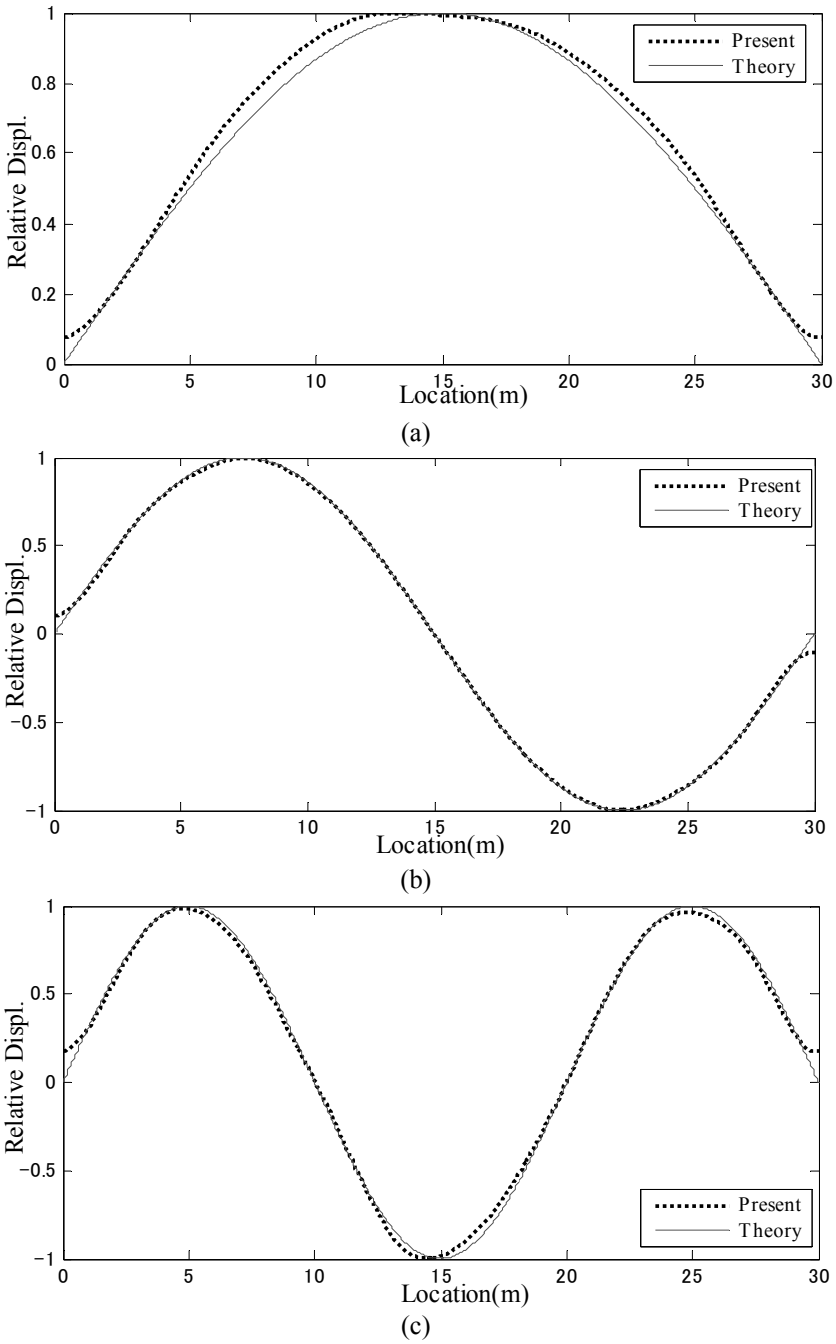


Fig. 8 Mode shapes of the bridge obtained by the present approach and theoretical formulae: (a) 1st mode, (b) 2nd mode and (c) 3rd mode

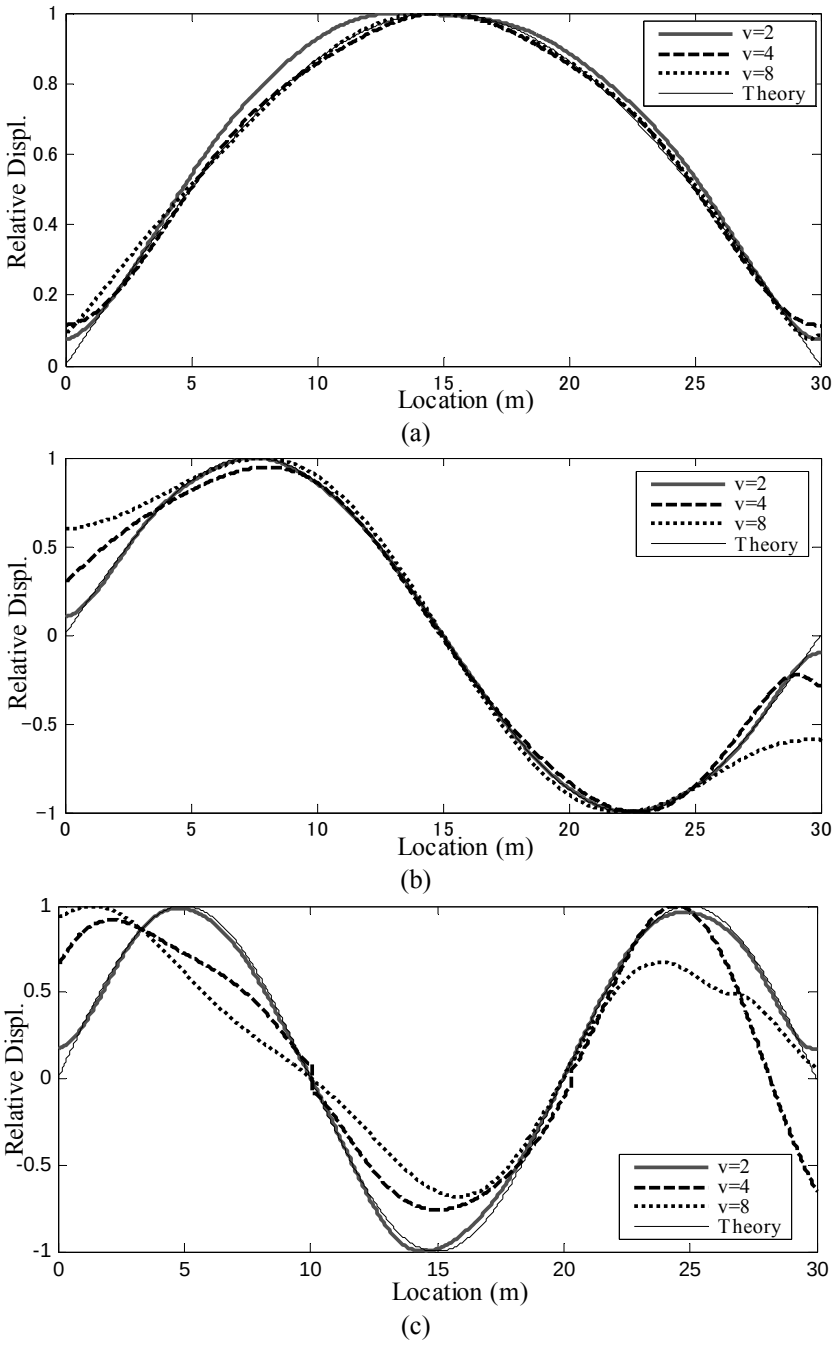


Fig. 9 Mode shapes of the bridge obtained for different vehicle speed: (a) 1st mode, (b) 2nd mode and (c) 3rd mode

Table 1 MAC of the first three modes for different vehicle speeds

| Speed (m/s) | 1st mode | 2nd mode | 3rd mode |
|---|---|---|---|
| 2 | 0.9984 | 0.9999 | 0.9981 |
| 4 | 0.9998 | 0.9955 | 0.8858 |
| 8 | 0.9997 | 0.9790 | 0.6824 |

If the vehicle moves at a low speed, say 2 m/s, the three extracted mode shapes match very well with the theoretical ones, generally with MAC values over 0.998. As the vehicle speed is doubled to 4 m/s or twice doubled to 8 m/s, the 1st extracted mode shapes show little deviation from the theoretical ones, still with MAC values over 0.998. However, the 2nd extracted mode shapes show slight deviations, with larger deviations concentrated at the end nodes, and the MAC value decreases as the vehicle speed increases. The 3rd mode shapes show obvious deviations, also with decreasing MAC values as the vehicle speed increases. It is concluded herein that a lower vehicle speed guarantees higher accuracy of the extracted mode shapes of a bridge, which is especially true for the higher modes. Such a conclusion is consistent with the suggestion made in the previous section. In addition, the larger discrepancy in identified mode shapes at the supports is also consistent with the discussion in the previous section: the theoretical amplification factor $R_m$ is sensitive in the vicinity of nodal points, and non-sensitive in the vicinity of peaks or troughs of the mode shape.

Table 2 Properties of random traffic

| Vehicle Number | Mass (kg) | Stiffness (N/m) | Speed (m/s) | Initial spacing (m)* | Remark |
|---|---|---|---|---|---|
| 1 | 1000 | 170000 | 2 | 0 | Test Vehicle |
| 2 | 1000 | 170000 | random | 1 | |
| 3 | 1000 | 170000 | random | 3 | |
| 4 | 1000 | 170000 | random | 5 | |

Note: *Initial spacing denotes the spacing between the accompanying vehicle and test vehicle at the instant when the test vehicle enters the bridge

### *5.3 Test vehicle traveling along with random traffic*

Except for the test vehicle, three accompanying vehicles moving at random speeds are considered to simulate the effect of random traffic, whose dynamic properties have been assigned, as listed in Table 2.

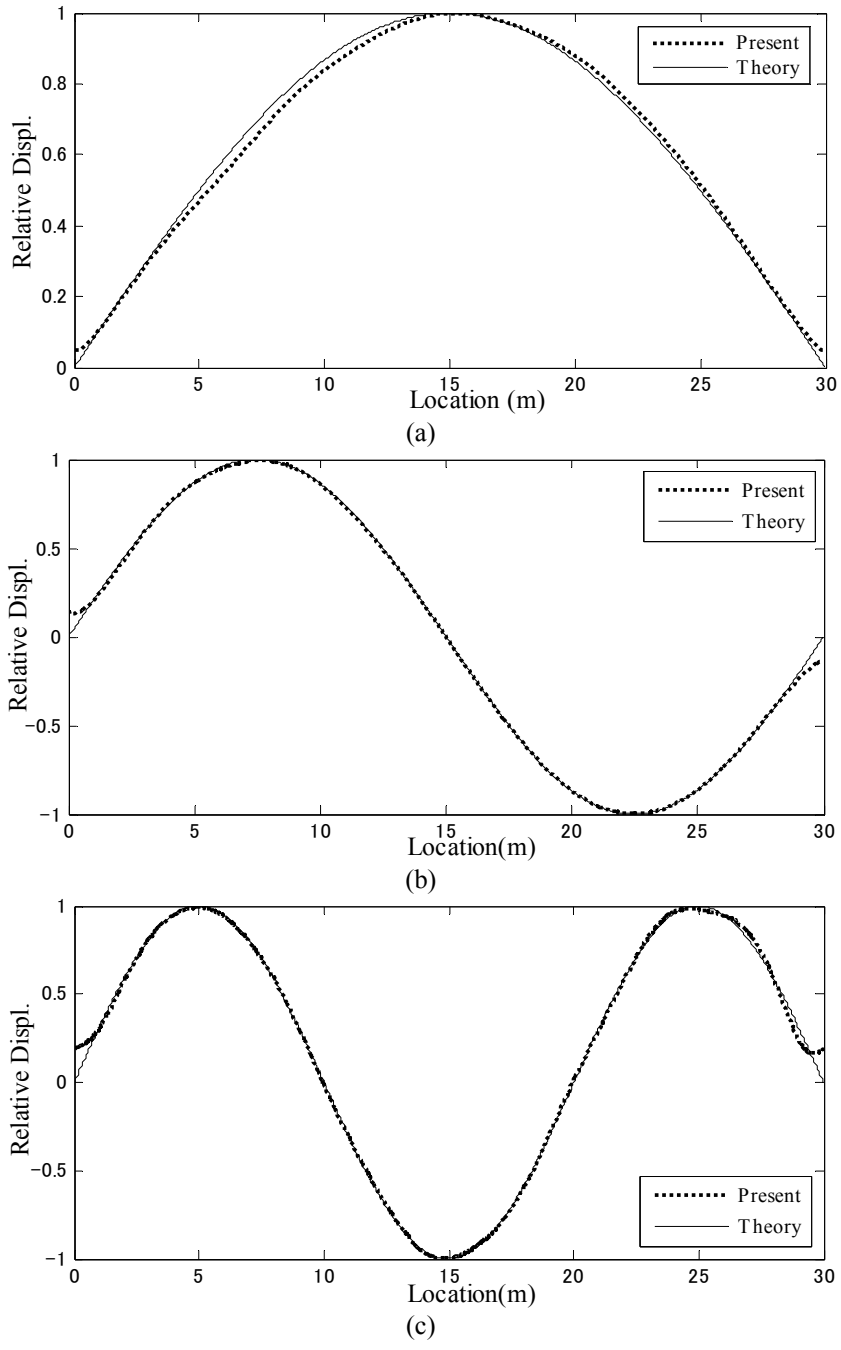


Fig. 10 Mode shapes of the bridge obtained from a test vehicle traveling with random traffic: (a) 1st mode, (b) 2nd mode and (c) 3rd mode

The first three extracted mode shapes of the bridge for this case are shown in Fig. 10. In comparison with the theoretical mode shapes, the extracted ones show high accuracy, with an MAC value of 0.9990 for the 1st mode, 0.999 for the 2nd mode, and 0.9994 for the 3rd mode. It is observed that the random traffic of the pattern presented in this section can hardly affect the accuracy of the extracted mode shapes of the bridge, possibly because the mass of the vehicles are too small to affect the bridge mode shapes.

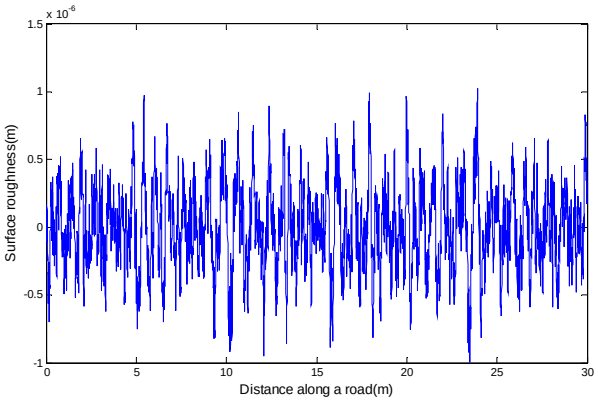


(a)

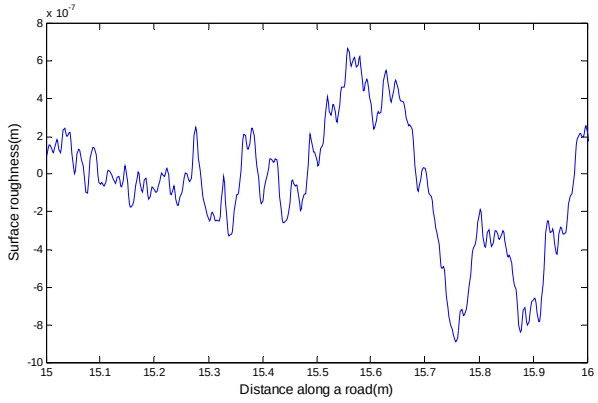


(b)

Fig. 11 Road surface roughness profile: (a) full span and (b) a close-up in the interval of 15-16 m

### *5.4 Effect of road surface roughness*

In this case, the effect of road surface roughness is studied by letting the test vehicle pass through a bridge with rough road surface. The road surface roughness is generated according to the power spectrum density (PSD) curve of class A presented by International Organization for Standardization (1995). Fig. 11 shows the generated road surface roughness profile that is adopted in this case.

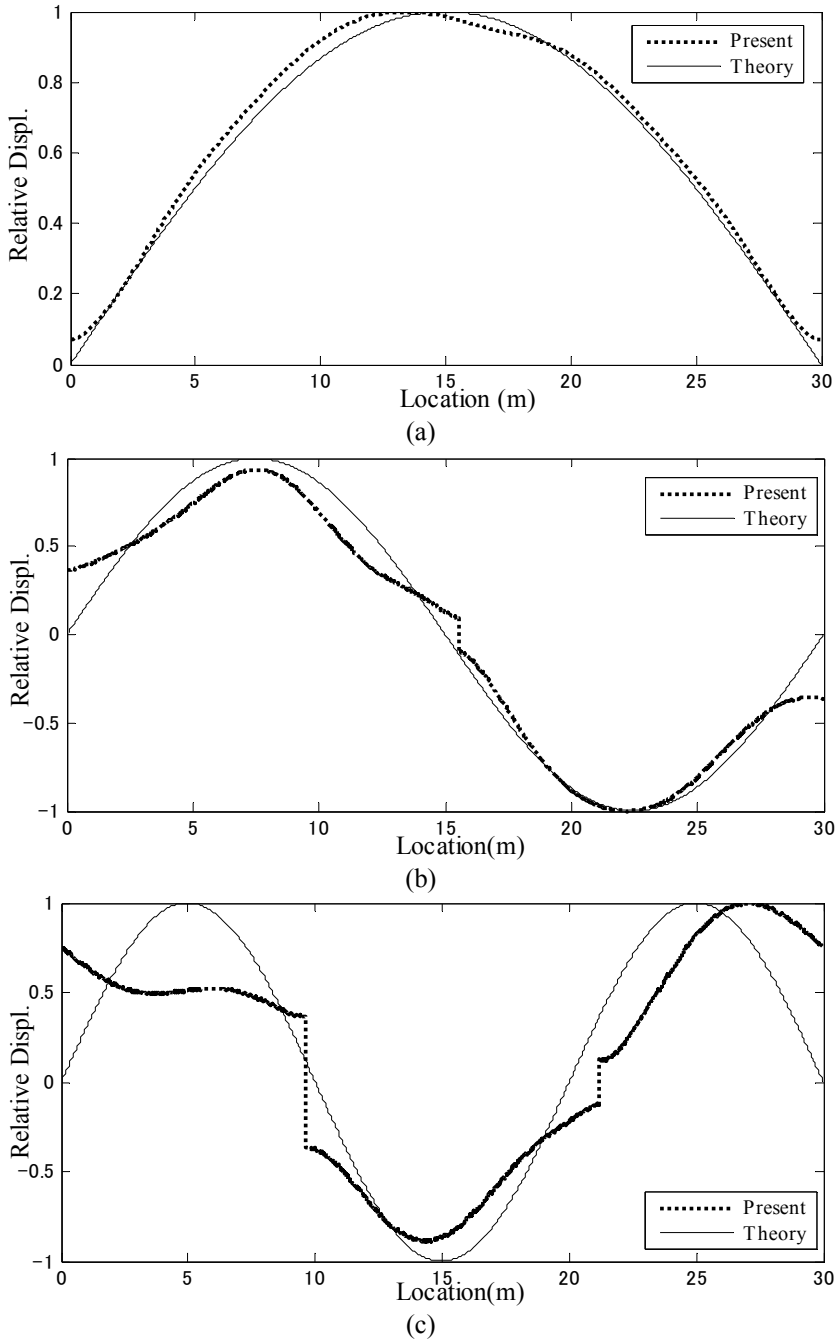


Fig. 12 Mode shapes of the bridge obtained from a test vehicle traveling on rough road surface: (a) 1st mode, (b) 2nd mode and (c) 3rd mode

Letting the test vehicle pass over the bridge with surface roughness of the above profile and then processing the dynamic responses of the test vehicle with the present algorithm, one can extract the mode shapes of the bridge as shown in Fig. 12. As can be seen, obvious distortions appear in the extracted mode shapes, especially for the 2nd and 3rd modes. The MAC value between the extracted mode shape and corresponding theoretical one is 0.9980 for the 1st mode, 0.9858 for the 2nd mode, and 0.7957 for the 3rd mode, all of which are smaller than those for the case with smooth road surface. Therefore, it is concluded that the existence of road surface roughness has negative impact on extracting the mode shapes of the bridge by the present approach, especially for the higher modes. In addition, discontinuity occurs at the nodes, as can be observed from the values for the same nodes with different signs.

The reasons for the negative impact of road surface roughness on the extraction of mode shapes can be given as follows. Firstly, the present approach for extracting the mode shapes of the bridge is based on the assumption that the bridge frequencies have been identified from the dynamic response of the test vehicle. The latter is known to be negatively impacted by the existence of road surface roughness (Chang *et al*. 2010). It follows that the former is also impacted. Secondly, during its passage over the bridge, the test vehicle is excited by both the vibrations of the bridge and the road surface roughness. The bridge vibrates with fixed modal frequencies and shapes, while the road surface roughness injects a wide range of spatial frequency into the vehicle response. Clearly, the mode shapes of the vibrating bridge mingle with the surface roughness profile of the frequency identical or close to the bridge frequency of interest. The mingled mode shapes and surface roughness profile are hardly to be separated by the frequency-domain filtering techniques, thereby making the extracted mode shapes distorted. Thirdly, such a distortion is more severe for higher modes since the amplitudes of higher modes are generally smaller than those of lower modes and thus easier to mingle with surface roughness profiles.

## 6. Conclusions

This study presents an indirect approach for extracting the mode shapes of a bridge from a passing test vehicle. Based on the theoretical formulation, it is observed that in the vibration response of the test vehicle during its passage over the bridge, the component response of the bridge frequency of certain mode oscillates with a varying amplitude that is identical to the mode shape of the bridge of the mode of concern. Therefore, once a bridge frequency is identified and its corresponding component response is separated from the vehicle response, the instantaneous amplitude history of the extracted component response can be regarded as a representative of the mode shape of the bridge. Theoretically, the mode shapes can be extracted with a high resolution in space since each point of the bridge is passed through by the test vehicle.

Through numerical case study, the present approach is verified to be feasible under the constraint that the vehicle speed is constant and low, say as low as 2 m/s. Also, the impact of the following factors on the accuracy of the extracted mode shapes is evaluated. (1) Vehicle speed: Lower vehicle speeds generally guarantee higher accuracy of the mode shapes, which is especially true for the second and third modes. (2) Random traffic: it can hardly affect the accuracy of the mode shapes. (3) Road surface roughness: The existence of road surface roughness has negative impact on extracting the mode shapes, especially for the higher modes.

The conclusions drawn herein are based on analytical derivations and numerical simulations, which should be further verified with experiments in field or laboratories before practical

applications. Future research should continue on techniques to remove the constraint on the constant and low vehicle speed, and the negative impact of road surface roughness on the extracted mode shapes.

## Acknowledgements

The research reported herein is partly sponsored by the National Science Council through Grant No. NSC 100-2221-E-224-045-MY2 to the first author and NSC 100-2917-I-564-052 to the third author K.C. Chang for his postdoctoral study. Such financial aids are gratefully acknowledged. The assistance from Tongji University (973 program, Ministry of Science and Technology, PRC) should also be acknowledged.

## References

Altunisik, A.C, Bayraktar, A. and Özdemir, H. (2012), "Seismic safety assessment of eynel highway steel bridge using ambient vibration measurements", *Smart Struct. Syst*., **10**(2), 131-154.

Bandat, J.S. and Piersol, A.G. (1986), *Random Data: Analysis and Measurement Procedures,* 2nd Ed., John Wiley & Sons, Inc., New York.

Brownjohn, J.M.W., Xia, P.Q., Hao, H. and Xia, Y. (2001), "Civil structure condition assessment by FE model updating: methodology and case studies", *Finite Elem. Anal. Des*., **37**(10), 761-775.

Bu, J.Q., Law, S.S. and Zhu, X.Q. (2006), "Innovative bridge condition assessment from dynamic response of a passing vehicle", *J. Eng. Mech. - ASCE*, **132**(12), 1372-1379.

Carden, E.P. and Fanning, P. (2004), "Vibration-based condition monitoring: a review", *Struct. Health Monit.*, **3**(4), 355-377.

Chang, P.C., Flatau, A. and Liu, S.C. (2003), "Review paper: Health monitoring of civil infrastructure", *Struct. Health Monit.*, **2**(3), 257-267.

Chang,K.C., Wu, F.B. and Yang, Y.B. (2010), "Effect of road surface roughness on indirect approach for measuring bridge frequencies from a passing vehicle", *Interact. Multiscale Mech*., **3**(4), 299-308.

Chrysostomou, C.Z., Demetriou, T. and Stassis, A. (2008), "Health-monitoring and system-identification of an ancient aqueduct", *Smart Struct. Syst*., **4**(2), 183-104.

Clough, R.W. and Penzien, J. (1993), *Dynamics of structures*, 2nd Ed., Mcgraw-Hill Book Co., Singapore.

Doebling, S.W., Farrar, C.R., and Prime, M.B. (1998), "A summary review of vibration-based damage identification methods", *Shock Vib. Digest*, **30**, 91-105.

Ewins, D.J. (2000), *Modal testing: theory, practice and application*, 2nd Ed, Research Studies Press, Ltd., England.

Fang, S.E. and Perera, R. (2009), "Power mode shapes for early damage detection in linear structures", *J. Sound Vib.*, **324**(1-2), 40-56

Farrar, C.R., Doebling, S.W. and Nix, D.A. (2001), "Vibration-based structural damage identification", *Philos. T. R. Soc. Lond. A*, **359**, 131-149.

Farrar and James (1997), "System identification from ambient vibration measurements on a bridge", *J. Sound Vib.*, **205**(1), 1-18.

Huang, C.S., Yang, Y.B., Lu, L.Y. and Chen, C.H. (1999), "Dynamic testing and system identification of a multi-span highway bridge", *Earthq. Eng. Struct. D.*, **28**(8), 857-878.

Huang, N.E., Shen, Z., Long, S.R., Wu, M.C., Shih, H.H., Zheng, Q. Yeh, N.C., Tung, C.C. and Liu, H.H. (1998), "The empirical mode decomposition and the Hilbert spectrum for nonlinear and non-stationary time series analysis", *Proc. R. Soc. Lond. A*, **454**, 903-995.

Huang, N.E., Shen, Z. and Long, S.R. (1999), "A new view of nonlinear water waves: the Hilbert spectrum", *Annu. Rev. Fluid Mech.*, **31**, 417-457.
International Organization for Standardization (ISO) (1995), Mechanical vibration – road surface profiles – reporting of measured data, ISO 8608.
Jaishi, B. and Ren, W.X. (2005), "Structural finite element model updating using ambient vibration test results", *J. Struct. Eng. - ASCE*, **131**(4), 617-628.
McGetrick, P.J., Gonzalez, A. and OBrien, E.J. (2009), "Theoretical investigation of the use of a moving vehicle to identify bridge dynamic parameters", *Insight*, **51**(8), 433-438.
Wenzel, H. and Pichler, P. (2005), *Ambient vibration monitoring*, John Wiley & Sons Ltd., England.
Yang, Y.B. and Chang, K.C. (2009), "Extraction of bridge frequencies from the dynamic response of a passing vehicle enhanced by the EMD technique", *J. Sound Vib.*, **322**(4-5), 718-739.
Yang, Y.B., Lin, C.W. and Yau, J.D. (2004), "Extracting bridge frequencies from the dynamic response of a passing vehicle", *J. Sound Vib.*, **272**(3-5), 471-493.
Yang, Y.B. and Lin, C.W. (2005), "Vehicle-bridge interaction dynamics and potential applications", *J. Sound Vib.*, **284**(1-2), 205-226.
Yang, Y.B. and Yau, J.D. (1997), "Vehicle-bridge interaction element for dynamic analysis", *J. Struct. Eng. - ASCE*, **123**(11), 1512-1518.
Yang, Y.B., Yau, J.D. and Wu, Y.S. (2004), *Vehicle-bridge interaction dynamics: with applications to high-speed railways*, World Scientific Publishing Co., Singapore.
Yin, S.H. and Tang, C.Y. (2011), "Identifying cable tension loss and deck damage in a cable-stayed bridge using a moving vehicle", *J. Vib. Acoust.*, **133**(2), 021007.
Zhang, Y., Wang, L. and Xiang, Z. (2012), "Damage detection by mode shape squares extracted from a passing vehicle", *J. Sound Vib.*, **331**(2), 291-307.